



Contents lists available at ScienceDirect

## European Journal of Medicinal Chemistry

journal homepage: <http://www.elsevier.com/locate/ejmech>

Original article

# Macrocyclic compounds as anti-cancer agents: Design and synthesis of multi-acting inhibitors against HDAC, FLT3 and JAK2



Cheng-Qing Ning<sup>a</sup>, Cheng Lu<sup>a</sup>, Liang Hu<sup>a</sup>, Yan-Jing Bi<sup>a</sup>, Lei Yao<sup>a</sup>, Yu-Jun He<sup>a</sup>, Li-Fei Liu<sup>a</sup>, Xiao-Yu Liu<sup>a, b, \*\*, \*</sup>, Nie-Fang Yu<sup>a, \*</sup>

<sup>a</sup> School of Pharmaceutical Sciences, Central South University, Changsha 410013, China<sup>b</sup> Drug Discovery Department, Hisun Group, Taizhou 317700, China

## ARTICLE INFO

## Article history:

Received 12 November 2014

Received in revised form

22 January 2015

Accepted 13 March 2015

Available online 17 March 2015

## ABSTRACT

A novel series of macrocyclic compounds were designed and synthesized as multi-target inhibitors targeting HDAC, FLT3 and JAK2. Some of these compounds exhibited potent HDAC inhibition as well as FLT3 and JAK2 inhibition under both cell-free and cellular conditions. *In vitro* antiproliferative assay indicated that these compounds were interestingly more cytotoxic to MV4-11 cells bearing FLT3-ITD mutation and HEL cells bearing JAK2<sup>V617F</sup> mutation.

© 2015 Elsevier Masson SAS. All rights reserved.

## Keywords:

Histone deacetylase

FLT3

JAK2

Macrocyclic

Multi-target inhibitor

## 1. Introduction

Acute myeloid leukemia (AML) is characterized by aberrant proliferation of myeloid cells in the marrow and an arrest in their maturation, which typically leads to death within weeks to months if left untreated [1,2]. The standard treatment for patients with AML is still chemotherapy regimens including cytarabine and an anthracycline (such as daunorubicin), which can produce a complete remission in almost 70% of patients. However, most patients will ultimately relapse and finally die of their disease within 2 years of achieving first remission [2,3]. Due to the high incidence of relapse and poor prognosis, new strategies for treatment of AML are warranted. In recent years, with the growing understanding of the pathophysiology and molecular biology of AML, the development of targeted therapies has led to promising results against AML. Well-explored targets in these therapies include histone deacetylases (HDACs), Fms-like tyrosine kinase 3 (FLT3) and Janus kinase 2 (JAK2), in particular their combination [2–6].

HDACs are a family of enzymes that regulate chromatin remodeling and gene transcription by catalyzing the deacetylation of the acetyl lysine residue on histone tails [7–9]. Inhibition of HDAC can impact a variety of cell functions by blocking the deacetylation of histone or non-histone proteins, such as p53, tubulin, and HSP90, causing cell cycle arrest, differentiation, and/or apoptosis [10]. FLT3 belongs to the class III of receptor tyrosine kinases, which control the development of hematopoietic progenitor cells [11]. It has been reported that more than two-third patients having AML highly expressed wild-type FLT3 and approximately one-third AML patients harbor FLT3 mutations [12]. The two major types of mutations that occur are internal tandem duplication (ITD) mutations of the juxtamembrane region and point mutations in the tyrosine kinase domain (TKD). Mutant FLT3 results in constitutive activation of the receptor's tyrosine kinase activity in the absence of ligand and is associated with poor prognosis of AML patients [2]. The Janus kinases (JAKs) are a family of non-receptor tyrosine kinases involved in cytokine signaling via the JAK-STAT pathway [13]. They play an important role in the pathogenesis of myeloid malignancies [14]. Most patients with myeloproliferative neoplasms (MPNs) harbor a somatic JAK2<sup>V617F</sup> mutation, resulting in constitutively activation of JAK-STAT pathway [6]. Also, JAK2 mutations have been found in patients with AML [15].

It has been reported that co-treatment with HDAC inhibitor

\* Corresponding author.

\*\* Corresponding author. School of Pharmaceutical Sciences, Central South University, Changsha 410013, China.

E-mail address: [niefang\\_yu@126.com](mailto:niefang_yu@126.com) (N.-F. Yu).

Panbinostat (SB939) and JAK2 inhibitor TG101209 could attenuate JAK2<sup>v617f</sup> levels and downstream signaling and induce synergistic apoptosis of MPD cells. It was demonstrated that treatment of JAK2<sup>v617f</sup> mutant cells with SB939 disrupted the chaperone association of JAK2<sup>v617f</sup> with HSP90, consequently promoting proteasomal degradation of JAK2<sup>v617f</sup> [16]. More recently, SB939 and FLT3/JAK2 inhibitor Pacritinib (SB1518) are reported to exert synergistic cytotoxic effects against cell lines carrying JAK2<sup>v617f</sup> mutation and FLT3-ITD mutation. The synergistic effects were attributed to impaired chaperone function of HSP90 by the HDAC inhibitor, since both JAK2 and FLT3 have been identified as HSP90 client proteins [17,18]. In addition, another recent report showed that HDAC inhibitors could selectively target FLT3-ITD for degradation in AML cells [12]. Thus, a combination therapy with an HDAC inhibitor and a JAK2/FLT3 inhibitor might be a promising approach for the treatment of AML, including those with FLT3 or JAK2 mutations. Herein, we report the first exploration of design, synthesis and evaluation of a single chemical entity that can simultaneously inhibit HDAC, FLT3, and JAK2.

The study was initiated by understanding the structural requirements of HDAC, FLT3 and JAK2 inhibitors. It has been well documented that the structural requirements of a typical HDAC inhibitor should include a zinc binding group to efficiently chelate the zinc ion, a linker to occupy the hydrophobic tubular channel, a cap for surface recognition and a unit connect the linker and cap (Scheme 1). The co-crystal structure of SAHA with HDAC-like protein (HDLP) reveals that SAHA binds by inserting its six-carbon-long aliphatic chain into the tube-like pocket through multiple contacts with hydrophobic residues, the terminal hydroxamic acid group coordinating the zinc at the bottom of the pocket to disrupt enzyme activity, the cap group at the other end makes contacts with residues at the pocket entrance [19]. From our previous extensive modeling studies [20,21], the cap region of HDLP appeared large enough to accommodate the macrocyclic skeleton of SB1317, a FLT3/JAK2 inhibitor now in phase I study for hematological malignancies (NCT01204164).

Docking studies reveal that SB1317 binds to both FLT3 and JAK2 through the hydrogen bond interactions with residues (Cys694 for FLT3 and Leu932 for JAK2) at the hinge region (see Fig. 1). The methyl substituent is solvent exposed and points directly toward a channel outside of the FLT3 and JAK2 binding pocket. It is presumably that this methyl could be properly replaced without much disruption of binding affinity. Interestingly, this observation might be supported by the fact that a side chain of SB1518 appears in this nearby region of FLT3/JAK2 (Fig. 2) [22]. Therefore, the amino basic

centre may be a suitable connecting point to introduce a group containing a side-chain of a certain length that terminates with a hydroxamic acid for HDAC binding, without sacrificing FLT3/JAK2 binding affinity at the same time. Thus, series of target compounds were carefully constructed by combining these structural features based on macrocycle templates of SB1317 and SB1518 (Scheme 2).

## 2. Results and discussion

### 2.1. Chemistry

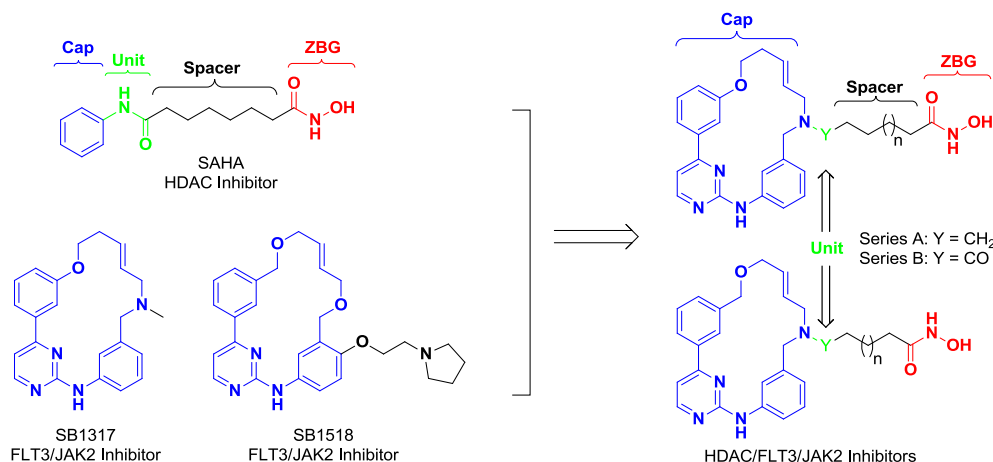
The preparation of macrocycles with various chain lengths is shown in Schemes 2 and 3 [21–24]. Scheme 2 describes the synthetic routes for intermediates **6**, **7** and **11**, and Scheme 3 illustrates the synthetic routes for macrocycles **30–41**.

As shown in Scheme 2, Compounds **4–5** were prepared through the Suzuki coupling of 2,4-dichloropyrimidine (**1**) with either boronic acids **2** or **3**. Alkylation of phenol **2** or phenylmethanol **3** with allyl bromide in the presence of base or phase transfer catalyst, gave the allyl ethers **6–7**. Coupling of 3-nitrobenzaldehyde (**8**) with allyl amine in the presence of NaBH(OAc)<sub>3</sub> gave the nitrobenzene **9**, which was subsequently reduced by Tin (II) chloride dehydrate, giving the aniline **10**. Then, the secondary amine was selectively N-Boc protected (**11**) by using a (Boc)<sub>2</sub>O/NaOH system.

Coupling of aniline **11** with chloropyrimidines (**6** or **7**) gave the corresponding dienes **12–13** as shown in Scheme 3. Compound **14–15** were obtained through ring-closing metathesis (RCM) of the dienes **12–13** in the presence of Grubbs second generation catalyst in moderate to good yields. The Boc-group was then removed in the presence of trifluoroacetic acid, which gave the key intermediates **16–17**. The corresponding side chain attached to the macrocycle was introduced using a coupling reaction. For example, compound **16–17** can be converted to intermediates **18–20** and **24–26** in high conversion rate by reacting with corresponding aldehydes under the aforementioned NaBH(OAc)<sub>3</sub> conditions, while the amines **16–17** can be also converted to intermediates **21–23** and **27–29** by coupling with the corresponding carboxylic acids in the presence of DIC and DMAP in high conversion rate. Finally, the intermediates were converted to hydroxamates **30–41** in moderate to good yields, using NH<sub>2</sub>OH·HCl/MeONa/MeOH system, a standard procedure developed in our lab.

### 2.2. In vitro enzymatic inhibitory activities

The enzymatic inhibitory activities of the target compounds



Scheme 1. Design of multi-target inhibitors against HDAC, FLT3 and JAK2.

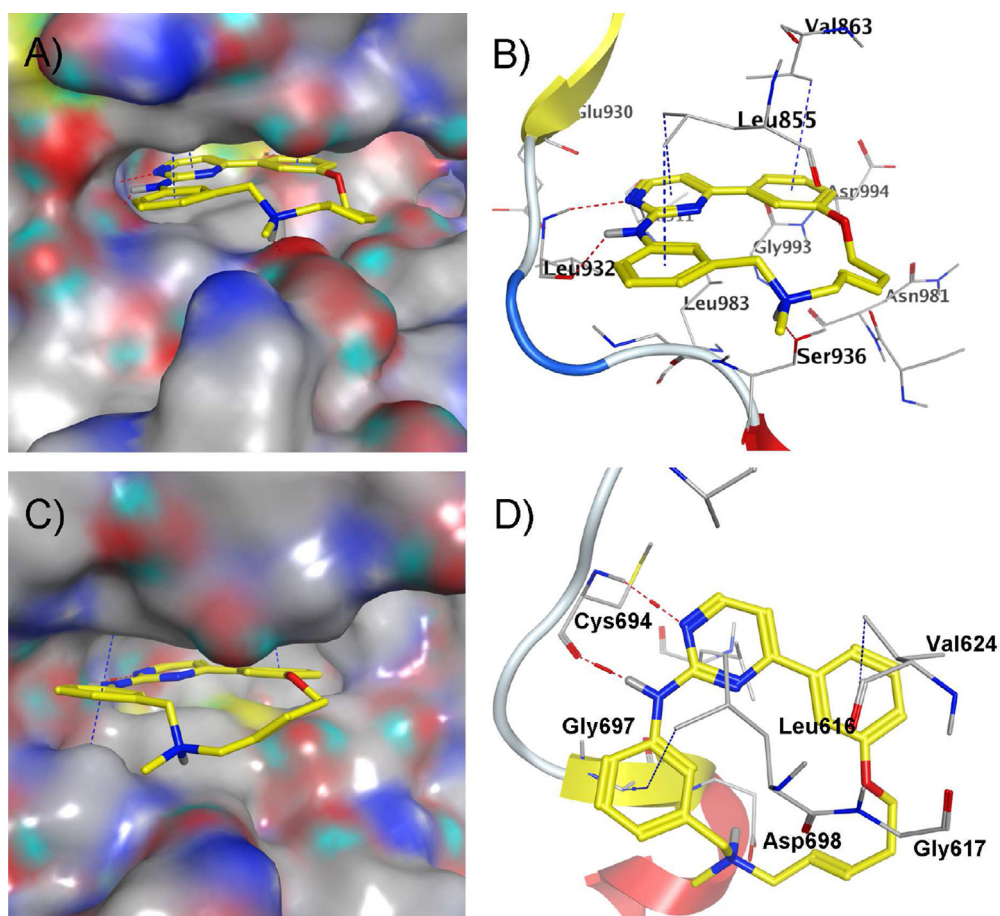


**Fig. 1.** SB1317 docked into JAK2 (PDB code: 2B7A) and FLT3 (PDB code: 1RJB). A–B), SB1317 docked into JAK2; C–D), SB1317 docked into FLT3. SB1317 is represented as yellow stick; the structure of hinge region is represented as a cartoon ribbon; H-bond and H- $\pi$  interactions are represented as red and blue dash line, respectively. (For interpretation of the references to colour in this figure legend, the reader is referred to the web version of this article.)

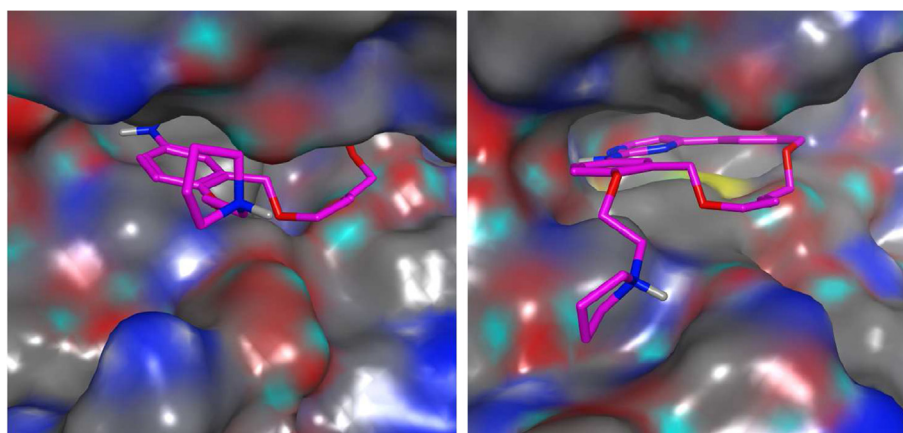


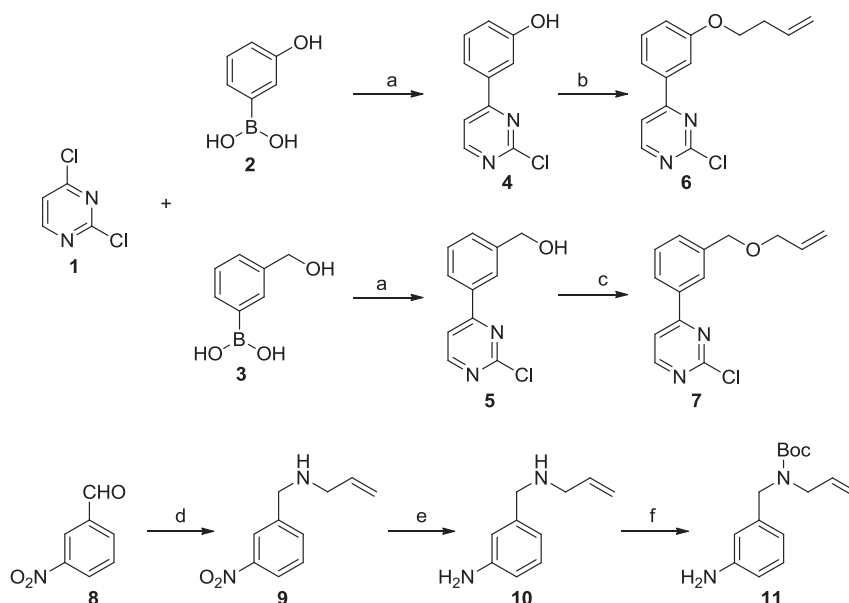
**Fig. 2.** The predicting binding pose of SB1518 (purple red, stick) in the pocket of JAK2 (left) and FLT3 (right). (For interpretation of the references to colour in this figure legend, the reader is referred to the web version of this article.)

were evaluated in FLT3 and JAK2 kinase activity assays, as well as an HDAC enzyme assay. The results were summarized in Table 1.

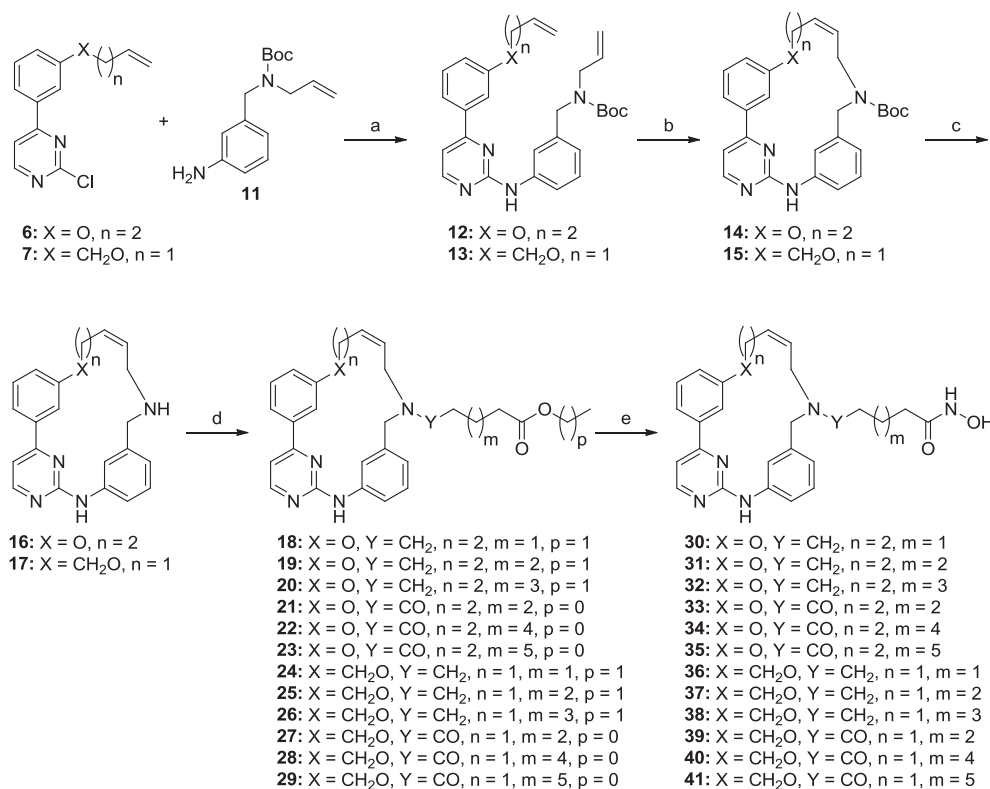
### 2.2.1. *In vitro* HDAC inhibition

As shown in Table 1, all the target compounds showed moderate to potent HDAC inhibitory activities, with  $IC_{50}$  values ranging from 87 to 848 nM. This suggests that both the macrocyclic moiety of

SB1317 and SB1518 are suitable cap groups for HDAC inhibitors. The enzymatic inhibitory activities of the tested compounds were marginally affected by the capping group, as indicated by the comparison between SB1317 hybrids (compounds 30–35) and their counterparts (SB1518 hybrids, compounds 36–40). In contrast, the data suggested that the unit Y were critical for HDAC inhibition. Obviously, stronger HDAC inhibitory activities were observed when



**Scheme 2.** Synthesis of intermediates **6**, **7** and **11**. Reagents and conditions: (a) Pd(PPh<sub>3</sub>)<sub>4</sub>, KF·2H<sub>2</sub>O, H<sub>2</sub>O, dioxane, 90 °C, 4 h; (b) 4-bromo-1-butene, Cs<sub>2</sub>CO<sub>3</sub>, DMF, 60 °C, overnight; (c) 3-bromopropene, KOH, n-Bu<sub>4</sub>NHSO<sub>4</sub>, CH<sub>3</sub>CN, 40 °C, overnight; (d) prop-2-en-1-amine, NaBH(OAc)<sub>3</sub>, DCM, 0 °C, 1 h; (e) SnCl<sub>2</sub>·2H<sub>2</sub>O, HAc:MeOH = 1:9, 60 °C, 5 h; (f) 4 N NaOH, (Boc)<sub>2</sub>O, r.t., overnight.

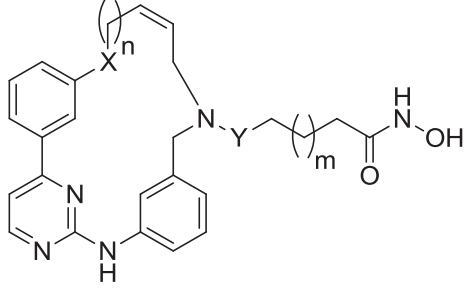


**Scheme 3.** Synthesis of target compounds **30–41**. Reagents and conditions: (a) Pd(PPh<sub>3</sub>)<sub>4</sub>, dppf, Cs<sub>2</sub>CO<sub>3</sub>, dioxane, 110 °C, 3 h; (b) Grubbs catalyst II, DCM, r.t., overnight; (c) TFA, DCM, r.t., 1 h; (d) oxo-alkyl-enoic acid ethyl ester, NaBH(OAc)<sub>3</sub>, DCM, 0 °C, 0.5–1 h or Alkyl-anedioic acid monomethyl ester, DIC, DMAP, DCM, r.t., 4–5 h; (e) NH<sub>2</sub>OH·HCl, MeONa, MeOH, 0 °C, 0.3–1 h.

the unit Y was a methylene group (series A: compounds **30–32** and **36–38**) compared to carbonyl group (series B: compounds **33–35** and **39–41**). The optimal carbon chain length seems to be five to six, which gives an IC<sub>50</sub> of HDAC inhibition similar to that of SAHA. Compound **32** exhibited the most potent HDAC inhibition, with an IC<sub>50</sub> value of 87 nM.

### 2.2.2. In vitro kinase inhibition

The target compounds tested exhibit moderate FLT3 and JAK2 inhibition compared to the reference compound SB1317. The data indicated that the unit Y was also critical for FLT3 inhibition. However, it seems not important for JAK2 inhibition. As shown in Table 1, series A (Y = –CH<sub>2</sub>–) showed higher activities against FLT3

**Table 1**  
*In vitro* enzyme inhibitory activities of target compounds.


Compds	X	Y	n	m	IC <sub>50</sub> (nM) <sup>a</sup>		
					HDAC <sup>b</sup>	FLT3 <sup>c</sup>	JAK2 <sup>d</sup>
<b>30</b>	O	CH <sub>2</sub>	2	1	251 ± 59	180 ± 9	293 ± 3
<b>31</b>	O	CH <sub>2</sub>	2	2	152 ± 21	108 ± 3	1044 ± 67
<b>32</b>	O	CH <sub>2</sub>	2	3	87 ± 10	87 ± 12	686 ± 28
<b>33</b>	O	CO	2	2	848 ± 118	556 ± 9	246 ± 7
<b>34</b>	O	CO	2	4	310 ± 11	1256 ± 213	558 ± 3
<b>35</b>	O	CO	2	5	355 ± 41	ND <sup>e</sup>	1475 ± 186
<b>36</b>	CH <sub>2</sub> O	CH <sub>2</sub>	1	1	158 ± 6	218 ± 3	392 ± 4
<b>37</b>	CH <sub>2</sub> O	CH <sub>2</sub>	1	2	123 ± 5	288 ± 10	594 ± 24
<b>38</b>	CH <sub>2</sub> O	CH <sub>2</sub>	1	3	159 ± 9	217 ± 14	613 ± 13
<b>39</b>	CH <sub>2</sub> O	CO	1	2	402 ± 12	221 ± 25	547 ± 10
<b>40</b>	CH <sub>2</sub> O	CO	1	4	293 ± 6	833 ± 24	684 ± 18
<b>41</b>	CH <sub>2</sub> O	CO	1	5	334 ± 12	272 ± 8	835 ± 20
SAHA	—	—	—	—	105 ± 16	>10,000	>10,000
SB1317	—	—	—	—	ND	42 ± 10	170 ± 17

<sup>a</sup> Values are expressed as means ± standard deviation of three independent experiments.

<sup>b</sup> HDAC inhibitory activities were determined using the Biomol *Flour de Lys* system.

<sup>c</sup> FLT3 kinase activities were determined using the LanthaScreen™ Eu kinase binding assay kit (Invitrogen).

<sup>d</sup> JAK2 Kinase activities were determined using the Z'-LYTE™ kinase assay kit (Invitrogen).

<sup>e</sup> ND = Not determined.

than the series B (Y = –CO–), while the two series showed similar JAK2 inhibition.

The data also indicated that the carbon chain length appeared to have some influence on the potency of FLT3 and JAK2 inhibition, which suggests that the hydroxamic acid at one end of the carbon chain should have some kind of interaction with the receptors of FLT3 and JAK2. However, the optimal carbon chain length for HDAC inhibition seems not favor FLT3 or JAK2 inhibition.

### 2.3. Cell growth inhibition

To explore the antiproliferative effect of the targeted compounds in leukemia cells, HL-60, MV4-11, K-562 and HEL cell lines were selected for evaluation. Among them, HL-60 is a FLT3 wild type AML cell line, while MV4-11 is a FLT3 internal tandem duplication (FLT3-ITD) positive AML cell line. K562 is a JAK2 wild type CML cell line, while HEL is a JAK2<sup>V617F</sup> positive erythroleukemia cell line. The results were summarized in Table 2.

As shown in Table 2, our data suggested that FLT3-ITD bearing MV4-11 cells and JAK2<sup>V617F</sup> bearing HEL cells were more sensitive to the target compounds. This may be because that FLT3-ITD or JAK2<sup>V617F</sup> expressing leukemia cells were more addicted to FLT3 or JAK2 signaling for proliferation and survival. Part of the target compounds exhibited similar or superior antiproliferative effect to SAHA and SB1317 in MV4-11 and HEL cells. Compound **32** exhibited the most potent antiproliferative activities against MV4-11 and HEL cells, with GI<sub>50</sub> value of 0.27 and 0.34 μM, respectively, which was lower than SAHA and SB1317. In contrary to its superior

**Table 2**  
*In vitro* anti-proliferative activities of target compounds.

Compds	GI <sub>50</sub> (μM) <sup>a</sup>			
	HL-60	MV4-11	K-562	HEL
<b>30</b>	3.03 ± 0.79	0.66 ± 0.13	2.45 ± 0.22	0.51 ± 0.03
<b>31</b>	2.62 ± 0.10	0.53 ± 0.06	2.32 ± 0.37	2.26 ± 0.82
<b>32</b>	1.03 ± 0.15	0.27 ± 0.11	1.02 ± 0.17	0.34 ± 0.10
<b>33</b>	1.27 ± 0.14	1.01 ± 0.11	1.44 ± 0.27	2.11 ± 0.09
<b>34</b>	6.73 ± 1.27	5.89 ± 0.57	4.79 ± 1.47	5.25 ± 0.75
<b>35</b>	1.95 ± 0.06	ND <sup>b</sup>	2.02 ± 0.27	6.26 ± 1.55
<b>36</b>	2.05 ± 0.44	0.37 ± 0.10	1.83 ± 0.93	0.49 ± 0.10
<b>37</b>	2.30 ± 0.38	0.52 ± 0.10	2.09 ± 0.29	0.68 ± 0.04
<b>38</b>	0.90 ± 0.11	0.32 ± 0.04	0.94 ± 0.27	0.70 ± 0.25
<b>39</b>	4.43 ± 1.08	2.06 ± 0.25	4.97 ± 0.13	2.94 ± 0.87
<b>40</b>	2.87 ± 0.22	1.41 ± 0.17	4.39 ± 1.42	5.03 ± 0.15
<b>41</b>	1.66 ± 0.13	0.78 ± 0.03	2.64 ± 0.28	4.78 ± 0.79
SAHA	0.55 ± 0.07	0.59 ± 0.13	0.52 ± 0.16	0.76 ± 0.24
SB1317	1.13 ± 0.26	0.66 ± 0.30	1.23 ± 0.26	0.79 ± 0.25

<sup>a</sup> Anti-proliferative activities against K-562, HL-60, MV4-11 and HEL were determined using the CellTiter-Glo Assay kit (Promega, Madison, WI, USA). Values are expressed as means ± standard deviation of three independent experiments.

<sup>b</sup> ND = Not determined.

antiproliferative effect, **32** demonstrated less potent inhibitory activities than SB1317 against FLT3 and JAK2. Thus, the greater cellular potency of **32** against MV4-11 and HEL cells may be attributed to the synergistic effects resulting from simultaneous inhibition of HDAC, FLT3 and JAK2.

To further explore the antitumor effect of these HDAC/FLT3/JAK2 inhibitors, some of the target compounds were selected for evaluation of anti-proliferative effects in solid tumor cells, including HCT-116 (colon), MCF-7(breast), MDA-MB-435 (melanoma), NCI-H460 (non-small cell lung) and Ovar-5 (Ovarian). As shown in Table 3, the selected compounds all exhibited similar cellular potencies to the positive compound SAHA, with GI<sub>50</sub> value ranging from 0.81 to 2.72 μM. It seemed that the cellular potency of these selected compounds against solid tumor cells were more consistent with their HDAC inhibitory activities. This may be because that FLT3 is expressed in hematopoietic stem/progenitor cells. Thus, compared to the moderate JAK2 inhibitory activities, the cytotoxicity of these selected compounds against solid tumor may be mainly due to their HDAC inhibitory activities. This data also suggested that the target compounds were more cytotoxic to MV4-11 and HEL leukemia cells, bearing FLT3-ITD and JAK<sup>V617F</sup> mutation, respectively.

### 2.4. Western blotting

We then explored whether these multi-acting compounds could inhibit HDAC, and FLT3 and JAK2 phosphorylation in cellular

**Table 3**  
*In vitro* anti-proliferative activities of selected compounds.

Compds	GI <sub>50</sub> (μM) <sup>a</sup>				
	HCT-116	MCF-7	MDA-MB-435	NCI-H460	Ovar-5
<b>30</b>	1.53 ± 0.34	1.13 ± 0.24	2.72 ± 0.03	1.77 ± 0.37	1.22 ± 0.12
<b>31</b>	1.33 ± 0.49	1.32 ± 0.28	2.63 ± 0.57	1.60 ± 0.43	1.42 ± 0.61
<b>32</b>	0.82 ± 0.05	0.95 ± 0.22	1.77 ± 0.08	1.07 ± 0.10	1.22 ± 0.19
<b>33</b>	1.59 ± 0.15	2.09 ± 0.28	2.41 ± 0.48	2.25 ± 0.19	1.52 ± 0.61
<b>36</b>	0.81 ± 0.24	1.07 ± 0.16	1.88 ± 0.37	1.42 ± 0.10	1.13 ± 0.03
<b>38</b>	0.90 ± 0.31	1.13 ± 0.13	1.50 ± 0.54	1.19 ± 0.26	1.42 ± 0.27
SAHA	1.04 ± 0.28	0.61 ± 0.23	1.18 ± 0.21	0.85 ± 0.14	1.78 ± 0.47

<sup>a</sup> Cancer cell lines were plated at 3000 cells per well in a 96-well flat-bottomed plate with varying concentrations of compounds. The cells were incubated with compounds for 48 h in a humidified atmosphere of 5% CO<sub>2</sub> at 37 °C. Growth inhibition was determined by an SRB assay. Values are expressed as means ± standard deviation of three independent experiments.

condition. For this purpose, Leukemia cell lines MV4-11 and HEL were treated with **32** at 0.1–0.5  $\mu\text{M}$  for 24 h. The whole-cell extracts were prepared and cellular proteins were then analyzed by western blots with antibodies specific for acetylated histone H3 and tubulin, phosphorylated FLT3 and JAK2. In MV4-11 cell line, compound **32** promoted acetylation of histone H3 and tubulin in a dose-dependent manner, and effectively decreased the phosphorylated level of FLT3 (Fig. 3). In HEL cell line, compound **32** treated also effectively decreased p-JAK2 level.

We also explored the effect of these multi-acting compounds on downstream pathway, including the phosphorylation of STAT5 and AKT. As shown in Fig. 4, compound **32** can inhibit the phosphorylation of STAT5 and AKT in a dose-dependent manner.

### 2.5. Docking studies

The possible binding modes of the macrocyclic compounds on HDAC, FLT3 and JAK2 were explored with the representative compounds **32** and **34** using MOE software. As illustrated by Fig. 5, compounds **32** and **34** binds to HDLP by inserting their aliphatic chains into the tube-like channel in a way similar as SAHA. The terminal hydroxamic acid group is coordinated with zinc ion at the bottom of the pocket. Obviously, the macrocyclic moiety at the other end of the aliphatic chain is well tolerated. Furthermore, in comparison to SAHA and compound **34**, an additional Hydrogen bond was observed between the aniline NH of **32** and Tyr264 residue. This may explain the stronger enzymatic inhibitory activity of compound **32** than that of **34** and SAHA.

Fig. 6 illustrates the predicted binding modes and detailed interactions of compound **32** and **34** with FLT3 and JAK2, respectively. Both compounds bind to the ATP binding site through hydrogen bonding between the amino-pyrimidine and residue at the hinge region. The side aliphatic chains form additional interactions with residues in the solvent-exposed area outside of the pocket. For FLT3, the backbone residue Cys694 participates in hydrogen bonding with amino-pyrimidine. Ser705 and Asn701 residues in the solvent-exposed area form electrostatic interactions with hydroxamate group in one end of the aliphatic chain. For JAK2, Leu932 residue in the hinge region participates in hydrogen bonding with amino-pyrimidine. In addition, hydrogen bond was observed between Leu932 and protonated amino basic central of compound **32**. In the case of compound **34**, an additional hydrogen bond was observed between hydroxamate group and Lys943 residue outside of the pocket. In general, this binding modes support our hypothesis that the methyl group of SB1317 could be properly replaced.

### 3. Conclusion

Novel macrocyclic compounds simultaneously inhibiting HDAC,

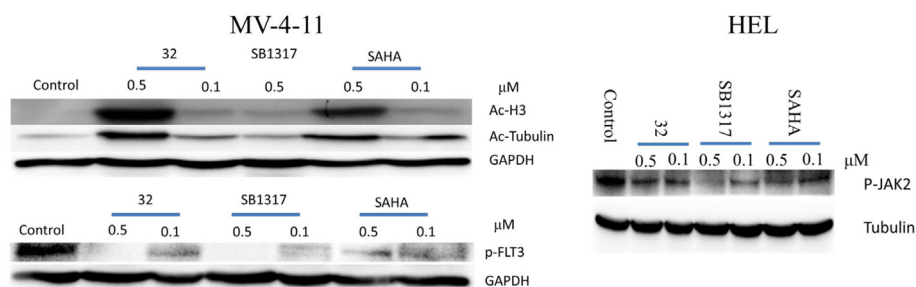


**Fig. 3.** Compound **32** induces acetylation of histone H3 and tubulin and downmodulates phosphorylated FLT3 and JAK2. The MV4-11 (FLT3-ITD) or HEL (JAK2<sup>V617F</sup>) cell lines were plated in the presence of indicated concentration of compound **32**. After 24 h of treatment, total cellular extracts were prepared and analyzed by western blots with antibodies specific for the indicated proteins.

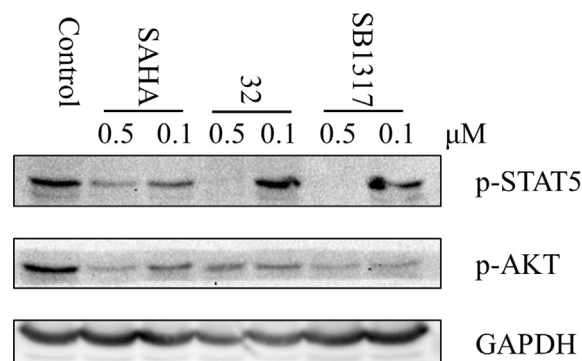


**Fig. 4.** Compound **32** decreases the expression of phosphorylated STAT5 and AKT. The MV4-11 cells were plated in the presence of indicated concentration of compound **32**. After 24 h of treatment, total cellular extracts were prepared and analyzed by western blots with antibodies specific for the indicated proteins.

FLT3 and JAK2 were conceived, synthesized, and evaluated *in vitro*. It was demonstrated that most of these macrocycles exhibited potent HDAC inhibition as well as FLT3 and JAK2 inhibition under both cell-free and cellular conditions. *In vitro* cell growth inhibition assays indicated that these multi-acting compounds were more cytotoxic to MV4-11 and HEL cells, bearing FLT3-ITD and JAK2<sup>V617F</sup> mutation, respectively. Compound **32** display promise as anticancer agent with the potential to treat AML patients with FLT3-ITD or JAK2<sup>V617F</sup> positive, and has been selected for further study as novel anticancer agent.

## 4. Experimental section

### 4.1. General

All moisture-sensitive reactions were performed in an inert atmosphere of dry nitrogen. Dichloromethane was distilled from CaH<sub>2</sub>. All other reagents and solvents purchased from commercial sources were used directly without further purification. The progress of reactions was monitored by LC-MS. All compounds were purified by recrystallization, column chromatography or reverse phase chromatography. Column chromatography was performed on silica gel (200–300 mesh). Reverse phase chromatography was performed on a Gilson-281 Pre-HPLC equipped with a C-18 column (Ultimate XB-C18, 5  $\mu\text{m}$ , 4.6 mm  $\times$  150 mm), using mobile phase A-acetonitrile and mobile phase B-water containing 0.1% TFA. Fractions containing the desired product were lyophilized or evaporated to dryness under vacuum to provide the dry compound. <sup>1</sup>HNMR spectra were recorded at 400 MHz and are reported in parts per million (ppm) on the  $\delta$  scale relative to tetramethylsilane as an internal standard. High-resolution mass spectrometry (HRMS) was

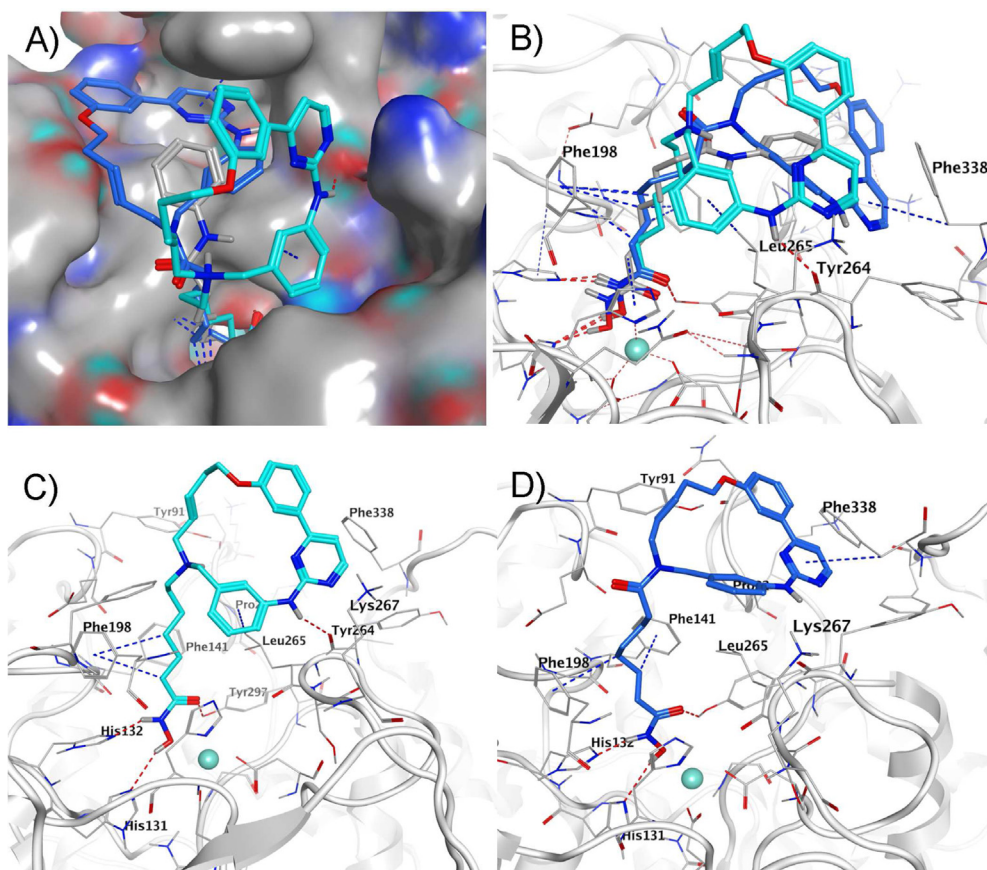


**Fig. 5.** Predicted binding modes of compounds **32** and **34** on HDLP (PDB code: 1C3S) and the detailed protein-inhibitor interactions. A) HDLP is shown as a surface; SAHA is shown as gray stick; compounds **32** is shown as cyan blue stick; compound **34** is shown as blue stick. B) SAHA, compounds **32** and **34** interacted with the active sites of HDLP. The hydrogen bond is represented as red dash line; the H- $\pi$  interaction is represented as blue dash line. C) Compound **32** interacted with the active sites of HDLP. D) Compound **34** interacted with the active site of HDLP. (For interpretation of the references to colour in this figure legend, the reader is referred to the web version of this article.)

performed on a Bruker MicroTOF QII instrument. The purity of the synthesized target compounds was determined to be  $\geq 95\%$  by HPLC, conducted on a Waters Xbridge-C18 column ( $4.6 \times 50$  mm,  $5 \mu\text{m}$ ).

## 4.2. Synthesis

### 4.2.1. 3-(2-Chloropyrimidin-4-yl)phenol (**4**)

To a degassed (nitrogen) solution of 2,4-dichloropyrimidine (10 g, 67.1 mmol) and (3-hydroxyphenyl)boronic acid (11.1 g, 80.5 mmol) in dioxane (100 mL) were added  $\text{KF} \cdot 2\text{H}_2\text{O}$  (25.5 g, 268.4 mmol),  $\text{Pd}(\text{PPh}_3)_4$  (5.4 g, 4.7 mmol) and 5 mL of water. The reaction mixture was heated at  $90^\circ\text{C}$  for 4 h. After cooling to room temperature, it was filtered and the filtrate was concentrated under reduced pressure to give the reddish-brown residue, which was purified by recrystallization from ethyl acetate. Compound **4** was obtained as a yellowish solid (8.5 g, 61.6%).  $^1\text{H NMR}$  (400 MHz,  $\text{DMSO}-d_6$ ,  $\delta$ ): 9.83 (s, 1H), 8.80 (d,  $J = 5.2$  Hz, 1H), 8.07 (d,  $J = 5.2$  Hz, 1H), 7.63–7.61 (m, 2H), 7.38 (t,  $J = 8.0$  Hz, 1H), 6.99 (ddd,  $J = 8.0$  Hz,  $J = 2.4$  Hz,  $J = 1.0$  Hz, 1H); MS  $m/z$ :  $[\text{M} + \text{H}]^+$  207.

### 4.2.2. (3-(2-chloropyrimidin-4-yl)phenyl)methanol (**5**)

The title compound was obtained as a yellow solid in 63.1% yield using a procedure similar to that of compound **4**.  $^1\text{H NMR}$  (400 MHz,  $\text{DMSO}-d_6$ ,  $\delta$ ): 8.83 (d,  $J = 5.2$  Hz, 1H), 8.17 (br, 1H), 8.14 (d,  $J = 5.2$  Hz, 1H), 8.06 (dt,  $J = 6.8$  Hz,  $J = 2.0$  Hz, 1H), 7.57–7.51 (m, 2H), 5.38 (br, 1H), 4.61 (s, 2H); MS  $m/z$ :  $[\text{M} + \text{H}]^+$  221.

### 4.2.3. 4-(3-(but-3-en-1-yloxy)phenyl)-2-chloropyrimidine (**6**)

A solution of **4** (6 g, 29 mmol) in DMF (100 mL) was treated with 4-bromo-1-butene (11.7 g, 87 mmol) and  $\text{Cs}_2\text{CO}_3$  (47.2 g, 145 mmol). The reaction mixture was heated at  $60^\circ\text{C}$  overnight. After cooling to room temperature, it was filtered and the filtrate was concentrated under high vacuum. The residue was purified by column chromatography (Hexane/EtOAc, 15:1) to afford **6** (6.6 g, 87.3%) as a white solid.  $^1\text{H NMR}$  (400 MHz,  $\text{DMSO}-d_6$ ,  $\delta$ ): 8.82 (d,  $J = 5.2$  Hz, 1H), 8.19 (d,  $J = 5.2$  Hz, 1H), 7.77 (d,  $J = 8.0$  Hz, 1H), 7.71 (t,  $J = 2.0$  Hz, 1H), 7.49 (t,  $J = 8.0$  Hz, 1H), 7.19 (dd,  $J = 8.0$  Hz,  $J = 2.0$  Hz, 1H), 5.97–5.87 (m, 1H), 5.22–5.09 (m, 2H), 4.14 (t,  $J = 6.8$  Hz, 2H), 2.55–2.51 (m, 2H); MS  $m/z$ :  $[\text{M} + \text{H}]^+$  261.

### 4.2.4. 4-(3-((allyloxy)methyl)phenyl)-2-chloropyrimidine (**7**)

A mixture of **5** (11 g, 49.9 mmol), KOH (9.8 g, 174.7 mmol), tetrabutylammonium hydrogen sulfate (1.2 g, 5 mmol), and 3-bromopropene (24.1 g, 199.6 mmol) in acetonitrile (150 mL) was heated at  $40^\circ\text{C}$  overnight. After cooling to room temperature, the reaction mixture was filtered and concentrated under reduced pressure. The residue was purified by column chromatography (Hexane/EtOAc, 7:1) to yield **7** (8.3 g, 63.8%) as a yellow solid.  $^1\text{H NMR}$  (400 MHz,  $\text{CDCl}_3$ ,  $\delta$ ): 8.64 (d,  $J = 7.2$  Hz, 1H), 8.08 (s, 1H), 8.03–8.00 (m, 1H), 7.66 (d,  $J = 7.2$  Hz, 1H), 7.56–7.50 (m, 2H), 6.03–5.94 (m, 1H), 5.37–5.22 (m, 2H), 4.61 (s, 2H), 4.09 (d,  $J = 7.2$  Hz, 2H); MS  $m/z$ :  $[\text{M} + \text{H}]^+$  261.

### 4.2.5. *tert*-butyl allyl(3-aminobenzyl)carbamate (**11**)

A mixture of 3-nitrobenzaldehyde (15.1 g, 0.1 mol) and prop-2-

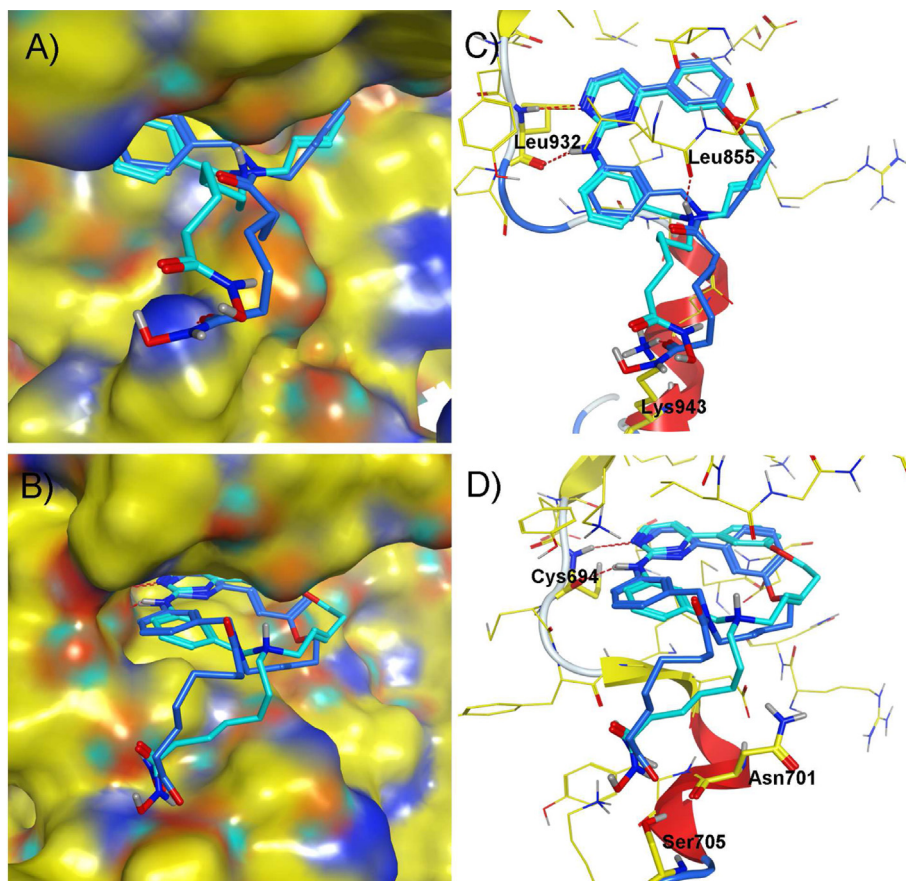


**Fig. 6.** Compounds **32** and **34** docked into JAK2 (A–B) and FLT3 (C–D). Compound **32**, cyan blue stick; Compound **34**, blue stick; H-bond, red dash line. (For interpretation of the references to colour in this figure legend, the reader is referred to the web version of this article.)

en-1-amine (8.6 g, 0.15 mol) in dichloromethane (250 mL) was stirred thoroughly. After cooling to 0 °C with an ice bath, NaBH(AcO)<sub>3</sub> (63.6 g, 0.3 mol) was added slowly. The resulting mixture was allowed to stir at room temperature for 1 h. The reaction mixture was quenched with water (200 mL) and extracted (DCM). The combined organic layers were dried (Na<sub>2</sub>SO<sub>4</sub>), concentrated under reduced pressure to provide a crude product, which was used in the next step without further purification.

The residue obtained above was dissolved in MeOH (252 mL). HAc (28 mL) and SnCl<sub>2</sub>·2H<sub>2</sub>O (67.7 g, 0.3 mol) was added. The resulting reaction mixture was stirred at 70 °C overnight, and then KOH/MeOH solution was added to adjust the pH ≈ 9. The resulting mixture was filtered, washed with DCM. The filtrate was condensed under reduced pressure, and then 150 mL DCM and 4 M NaOH aqueous solution (200 mL) were added. After cooling to 5 °C with an ice bath, (Boc)<sub>2</sub>O (0.08 mol) was added dropwise. The reaction mixture was allowed to stir at room temperature for 2 h. Then, it was extracted with DCM, dried over Na<sub>2</sub>SO<sub>4</sub>, filtered and concentrated under reduced pressure. The crude product was purified by column chromatography on silica gel using hexane/EtOAc (5:1) as eluent to afford the title compound as reddish-brown oil (14.9 g, 56.8%). <sup>1</sup>HNMR (400 MHz, DMSO-*d*<sub>6</sub>, δ): 6.95 (t, *J* = 8.0 Hz, 1H), 6.45–6.42 (m, 2H), 6.34 (d, *J* = 8.0 Hz, 1H), 5.78–5.68 (m, 1H), 5.12–5.04 (m, 4H), 4.19 (s, 2H), 3.72 (br, 1H), 3.67 (br, 1H), 1.41 (s, 9H); MS *m/z*: [M + Na]<sup>+</sup> 285.

#### 4.2.6. *tert*-butyl allyl(3-((4-(3-(*tert*-butyl-3-en-1-yloxy)phenyl)pyrimidin-2-yl)amino)benzyl)carb -amate (**12**)

To a degassed (nitrogen) solution of **6** (3 g, 11.5 mmol) and **11**

(3.3 g, 12.7 mmol) in dioxane (30 mL) were added Cs<sub>2</sub>CO<sub>3</sub> (15 g, 46 mmol), Pd(PPh<sub>3</sub>)<sub>4</sub> (1.6 g, 1.4 mmol) and dppf (1.3g, 2.3 mmol). The reaction mixture was heated at 110 °C for 3 h. After cooling to room temperature, it was filtered and the filtrate was concentrated under reduced pressure. The residue was purified by column chromatography (Hexane/EtOAc, 5:1) to yield **12** as orange-yellow oil (3.3 g, 58.9%). <sup>1</sup>HNMR (400 MHz, DMSO-*d*<sub>6</sub>, δ): 9.71 (s, 1H), 8.53 (d, *J* = 5.2 Hz, 1H), 7.72–7.67 (m, 4H), 7.46–7.40 (m, 2H), 7.27 (t, *J* = 7.6 Hz, 1H), 7.13 (dd, *J* = 7.2 Hz, *J* = 2.0 Hz, 1H), 6.83 (d, *J* = 7.6 Hz, 1H), 5.91 (m, 1H), 5.76 (m, 1H), 5.15 (m, 4H), 4.34 (br, 2H), 4.13 (t, *J* = 6.4 Hz, 2H), 3.80 (br, 1H), 3.74 (br, 1H), 2.54 (m, 2H), 1.39 (s, 9H); MS *m/z*: [M + H]<sup>+</sup> 488.

#### 4.2.7. *tert*-butyl allyl(3-((4-(3-((allyloxy)methyl)phenyl)pyrimidin-2-yl)amino)benzyl)carb -amate (**13**)

The title compound was obtained as orange-yellow oil in 51% yield using a procedure similar to that of compound **12**. <sup>1</sup>HNMR (400 MHz, DMSO-*d*<sub>6</sub>, δ): 8.46 (d, *J* = 7.2 Hz, 1H), 8.01 (m, 2H), 7.99 (br, 1H), 7.54–7.47 (m, 4H), 7.33–7.28 (m, 1H), 7.17 (d, *J* = 7.2 Hz, 1H), 6.93 (br, 1H), 6.04–5.91 (m, 1H), 5.77 (br, 1H), 5.37–5.08 (m, 4H), 4.61 (s, 2H), 4.45 (s, 2H), 4.08 (d, *J* = 6.4 Hz, 2H), 3.88 (br, 1H), 3.78 (br, 1H), 1.47 (s, 9H); MS *m/z*: [M + H]<sup>+</sup> 488.

#### 4.2.8. (16*E*)-14-*N*-Boc-20-oxa-5,7,14,26-tetraazatetracyclo[19.3.1.1(2,6)0.1(8,12)]heptacos-1(25),2(26),3,5,8(27),9,11,16,21,23-decaene (**14**)

A degassed (nitrogen) solution of **12** (3 g, 6.2 mmol) in dry DCM (450 mL) was heated to 45 °C with stirring. Then, the second generation Grubbs catalyst (764 mg, 0.9 mmol), predissolved in dry

DCM (15 mL), was added to the reaction mixture in three portions. The reaction mixture was stirred at reflux overnight. The solvent was removed under reduced pressure and subsequent purified by column chromatography (Hexane/EtOAc, 5:1) to yield **14** as a yellowish solid (2.2 g, 79%). <sup>1</sup>HNMR (400 MHz, DMSO-*d*<sub>6</sub>, δ): 9.77 (s, 1H), 8.56 (d, *J* = 5.2 Hz, 1H), 8.51 (s, 1H), 7.88 (s, 1H), 7.65 (d, *J* = 7.6 Hz, 1H), 7.46 (t, *J* = 7.6 Hz, 1H), 7.41 (d, *J* = 5.2 Hz, 1H), 7.29–7.23 (m, 2H), 7.09 (d, *J* = 8.0 Hz, 1H), 6.76 (d, *J* = 7.6 Hz, 1H), 5.62–5.55 (m, 1H), 5.41–5.35 (m, 1H), 4.89 (s, 2H), 4.58 (br, 2H), 4.15 (t, *J* = 5.2 Hz, 2H), 2.43 (m, 2H), 1.44 (s, 9H); MS *m/z*: [M + H]<sup>+</sup> 459.

4.2.9. (16E)-14-N-Boc-19-oxa-5,7,14,26-tetraazatetracyclo [19.3.1.1(2,6),1(8,12)]heptacos-1(25),2(26),3,5,8(27),9,11,16,21,23-decaene (**15**)

The title compound was obtained as a yellowish solid in 71% yield using a procedure similar to that of compound **14**. <sup>1</sup>HNMR (400 MHz, CDCl<sub>3</sub>, δ): 8.75 (s, 1H), 8.47–8.43 (m, 2H), 7.85–7.81 (m, 1H), 7.52–7.47 (m, 2H), 7.33–7.20 (m, 3H), 6.84–6.81 (m, 2H), 5.80–5.70 (m, 2H), 4.62 (s, 2H), 4.59 (s, 2H), 4.07 (d, *J* = 6.8 Hz, 2H), 3.91 (br, 2H), 1.53 (s, 9H); MS *m/z*: [M + H]<sup>+</sup> 459.

4.2.10. (16E)-20-oxa-5,7,14,26-tetraazatetracyclo [19.3.1.1(2,6),1(8,12)]heptacos-1(25),2(26),3,5,8(27),9,11,16,21,23-decaene (**16**)

A solution of **14** (2 g, 4.4 mmol) in DCM (20 mL) was added TFA (2 mL). The reaction mixture was stirred at room temperature for 1 h. The solvent was evaporated and the residue was dissolved in DCM (30 mL), washed by Na<sub>2</sub>CO<sub>3</sub> aqueous solution, dried over Na<sub>2</sub>SO<sub>4</sub>, and concentrated under reduced pressure to afford compound **16** as a yellowish solid (1.5 g, 97%). <sup>1</sup>HNMR (400 MHz, DMSO-*d*<sub>6</sub>, δ): 10.00 (s, 1H), 9.16 (br, 1H), 9.01 (s, 1H), 8.60 (d, *J* = 5.2 Hz, 1H), 7.94 (s, 1H), 7.64 (d, *J* = 8.0 Hz, 1H), 7.51 (d, *J* = 8.0 Hz, 1H), 7.48 (d, *J* = 5.2 Hz, 1H), 7.38 (t, *J* = 8.0 Hz, 1H), 7.28 (d, *J* = 8.0 Hz, 1H), 7.26 (td, *J* = 8.0 Hz, *J* = 2.4 Hz, 1H), 7.12 (d, *J* = 8.0 Hz, 1H), 6.10–6.03 (m, 1H), 5.71–5.64 (m, 1H), 4.23 (t, *J* = 5.2 Hz, 2H), 4.12–4.09 (m, 2H), 3.73 (br, 2H), 2.58–2.54 (m, 2H); MS *m/z*: [M + H]<sup>+</sup> 359.

4.2.11. (16E)-19-oxa-5,7,14,26-tetraazatetracyclo [19.3.1.1(2,6),1(8,12)]heptacos-1(25),2(26),3,5,8(27),9,11,16,21,23-decaene (**17**)

The title compound was obtained as a yellowish solid in 94% yield using a procedure similar to that of compound **16**. <sup>1</sup>HNMR (400 MHz, CDCl<sub>3</sub>, δ): 8.81 (s, 1H), 8.45 (d, *J* = 4.8 Hz, 1H), 7.83 (d, *J* = 7.6 Hz, 1H), 7.59 (d, *J* = 7.6 Hz, 1H), 7.51–7.48 (m, 1H), 7.30–7.26 (m, 2H), 7.21 (d, *J* = 5.2 Hz, 1H), 7.08 (d, *J* = 7.2 Hz, 1H), 6.81 (d, *J* = 8.0 Hz, 1H), 5.79–5.76 (m, 2H), 4.64 (s, 2H), 4.08 (d, *J* = 4.0 Hz, 2H), 3.86 (s, 2H), 3.41 (d, *J* = 4.4 Hz, 2H), 1.82 (br, 1H); MS *m/z*: [M + H]<sup>+</sup> 359.

4.2.12. Ethyl 5-(7-oxa-macrocyclic-1-yl)pentanoate (**18**)

The title compound was prepared from **16** and ethyl 5-oxopentanoate using a procedure similar to that of compound **9**. The obtained crude product was used in next step without further purification. LC/MS (ESI positive mode) *m/z* [M + H]<sup>+</sup> 487.

4.2.13. Ethyl 6-(7-oxa-macrocyclic-1-yl)hexanoate (**19**)

The title compound was prepared from **16** and ethyl 6-oxohexanoate using a procedure similar to that of compound **9**. The obtained crude product was used in next step without further purification. LC/MS (ESI positive mode) *m/z* [M + H]<sup>+</sup> 501.

4.2.14. Ethyl 6-(7-oxa-macrocyclic-1-yl)heptanoate (**20**)

The title compound was prepared from **16** and ethyl 7-oxoheptanoate using a procedure similar to that of compound **9**.

The obtained crude product was used in next step without further purification. LC/MS (ESI positive mode) *m/z* [M + H]<sup>+</sup> 515.

4.2.15. Methyl 6-(7-oxa-macrocyclic-1-yl)-6-oxohexanoate (**21**)

To a solution of 6-methoxy-6-oxohexanoic acid (39 mg, 0.25 mmol) in DCM (5 mL) was added DIC (33 mg, 0.26 mmol) and stirred at room temperature for 10 min. Then, DMAP (13 mg, 0.11 mmol) and **16** (80 mg, 0.22 mmol) were added. After stirring at room temperature for 4 h, water (5 mL) was added and extracted (DCM). The combined organic layer was dried (Na<sub>2</sub>SO<sub>4</sub>), filtered, and concentrated under reduced pressure to afford the crude product, which was used in next step without further purification. LC/MS (ESI positive mode) *m/z* [M + H]<sup>+</sup> 501.

4.2.16. Methyl 8-(7-oxa-macrocyclic-1-yl)-8-oxooctanoate (**22**)

The title compound was prepared from **16** and 8-methoxy-8-oxooctanoic acid using a procedure similar to that of compound **21**. The obtained crude product was used in next step without further purification. LC/MS (ESI positive mode) *m/z* [M + H]<sup>+</sup> 529.

4.2.17. Methyl 9-(7-oxa-macrocyclic-1-yl)-9-oxononanoate (**23**)

The title compound was prepared from **16** and 9-methoxy-9-oxononanoic acid using a procedure similar to that of compound **21**. The obtained crude product was used in next step without further purification. LC/MS (ESI positive mode) *m/z* [M + H]<sup>+</sup> 543.

4.2.18. Ethyl 5-(6-oxa-macrocyclic-1-yl)pentanoate (**24**)

The title compound was prepared from **17** and ethyl 5-oxopentanoate using a procedure similar to that of compound **9**. The obtained crude product was used in next step without further purification. LC/MS (ESI positive mode) *m/z* [M + H]<sup>+</sup> 487.

4.2.19. Ethyl 6-(6-oxa-macrocyclic-1-yl)hexanoate (**25**)

The title compound was prepared from **17** and ethyl 6-oxohexanoate using a procedure similar to that of compound **9**. The obtained crude product was used in next step without further purification. LC/MS (ESI positive mode) *m/z* [M + H]<sup>+</sup> 501.

4.2.20. Ethyl 6-(6-oxa-macrocyclic-1-yl)heptanoate (**26**)

The title compound was prepared from **17** and ethyl 7-oxoheptanoate using a procedure similar to that of compound **9**. The obtained crude product was used in next step without further purification. LC/MS (ESI positive mode) *m/z* [M + H]<sup>+</sup> 515.

4.2.21. Methyl 6-(6-oxa-macrocyclic-1-yl)-6-oxohexanoate (**27**)

The title compound was prepared from **17** and 6-methoxy-6-oxohexanoic acid using a procedure similar to that of compound **21**. The obtained crude product was used in next step without further purification. LC/MS (ESI positive mode) *m/z* [M + H]<sup>+</sup> 501.

4.2.22. Methyl 8-(7-oxa-macrocyclic-1-yl)-8-oxooctanoate (**28**)

The title compound was prepared from **17** and 8-methoxy-8-oxooctanoic acid using a procedure similar to that of compound **21**. The obtained crude product was used in next step without further purification. LC/MS (ESI positive mode) *m/z* [M + H]<sup>+</sup> 530.

4.2.23. Methyl 9-(7-oxa-macrocyclic-1-yl)-9-oxononanoate (**29**)

The title compound was prepared from **17** and 9-methoxy-9-oxononanoic acid using a procedure similar to that of compound **21**. The obtained crude product was used in next step without further purification. LC/MS (ESI positive mode) *m/z* [M + H]<sup>+</sup> 543.

4.2.24. General procedure for the synthesis of the hydroxamic acids **30–41**

A solution of methyl esters or ethyl esters (0.2 mmol) in MeOH

(1 mL) was added  $\text{NH}_2\text{OH}\cdot\text{HCl}$  (5.6 mmol). After cooling to 0 °C with an ice bath,  $\text{NaOMe}$  solution in  $\text{MeOH}$  (25%, 6 mmol) was poured into the reaction mixture. The progress of reaction was monitored by LC-MS (15–60 min). The reaction was quenched by cold 6 N  $\text{HCl}$ , and the resulting mixture was centrifuged, and sentenced to prep-HPLC chromatography. The target compounds were obtained as yellow solid with yield from 30% to 65%.

**4.2.24.1. 5-(7-Oxa-macrocyclic-1-yl)-N-hydroxypentanamide (30).**  $^1\text{H NMR}$  (400 MHz,  $\text{DMSO}-d_6$ ,  $\delta$ ): 10.29 (br, 1H), 9.99 (s, 1H), 9.77 (br, 1H), 8.91 (s, 1H), 8.60 (d,  $J = 5.2$  Hz, 1H), 7.90 (s, 1H), 7.65 (d,  $J = 7.6$  Hz, 1H), 7.51–7.47 (m, 2H), 7.40 (t,  $J = 8.0$  Hz, 1H), 7.32 (d,  $J = 8.0$  Hz, 1H), 7.25 (dd,  $J = 8.0$  Hz,  $J = 2.4$  Hz, 1H), 7.16 (d,  $J = 7.6$  Hz, 1H), 6.20–6.13 (m, 1H), 5.82–5.74 (m, 1H), 4.59–4.56 (m, 1H), 4.26–4.23 (m, 2H), 4.05–3.99 (m, 2H), 3.85–3.82 (m, 1H), 2.93–2.83 (m, 2H), 2.59–2.56 (m, 2H), 1.80 (t,  $J = 7.2$  Hz, 2H), 1.70–1.68 (m, 1H), 1.41–1.36 (m, 1H), 1.27–1.15 (m, 2H); MS  $m/z$ :  $[\text{M} + \text{H}]^+$  474; HRMS ( $m/z$ ):  $[\text{M} + \text{H}]^+$  calcd for  $\text{C}_{27}\text{H}_{32}\text{N}_5\text{O}_3$ , 474.2500; found, 474.2487.

**4.2.24.2. 6-(7-Oxa-macrocyclic-1-yl)-N-hydroxyhexanamide (31).**  $^1\text{H NMR}$  (400 MHz,  $\text{DMSO}-d_6$ ,  $\delta$ ): 10.28 (br, 1H), 9.99 (s, 1H), 9.81 (br, 1H), 8.90 (s, 1H), 8.60 (d,  $J = 5.2$  Hz, 1H), 7.89 (s, 1H), 7.64 (d,  $J = 8.0$  Hz, 1H), 7.51–7.46 (m, 2H), 7.39 (t,  $J = 8.0$  Hz, 1H), 7.31 (d,  $J = 8.0$  Hz, 1H), 7.24 (dd,  $J = 8.0$  Hz,  $J = 2.4$  Hz, 1H), 7.16 (d,  $J = 7.6$  Hz, 1H), 6.20–6.13 (m, 1H), 5.83–5.76 (m, 1H), 4.60–4.57 (m, 1H), 4.27–4.18 (m, 2H), 4.07–4.00 (m, 2H), 3.88–3.81 (m, 1H), 2.91–2.79 (m, 2H), 2.59–2.58 (m, 2H), 1.75 (t,  $J = 7.2$  Hz, 2H), 1.32–1.23 (m, 4H), 0.99–0.87 (m, 2H); MS  $m/z$ :  $[\text{M} + \text{H}]^+$  488; HRMS ( $m/z$ ):  $[\text{M} + \text{H}]^+$  calcd for  $\text{C}_{28}\text{H}_{34}\text{N}_5\text{O}_3$ , 488.2656; found, 488.2664.

**4.2.24.3. 7-(7-Oxa-macrocyclic-1-yl)-N-hydroxyheptanamide (32).**  $^1\text{H NMR}$  (400 MHz,  $\text{DMSO}-d_6$ ,  $\delta$ ): 10.26 (br, 1H), 9.99 (s, 1H), 9.74 (br, 1H), 8.90 (s, 1H), 8.60 (d,  $J = 5.2$  Hz, 1H), 7.90 (t,  $J = 2.0$  Hz, 1H), 7.64 (d,  $J = 7.6$  Hz, 1H), 7.49 (t,  $J = 8.0$  Hz, 1H), 7.51–7.46 (m, 2H), 7.31 (dd,  $J = 8.0$  Hz,  $J = 2.4$  Hz, 1H), 7.23 (dd,  $J = 8.0$  Hz,  $J = 2.4$  Hz, 1H), 7.15 (d,  $J = 7.6$  Hz, 1H), 6.19–6.12 (m, 1H), 5.84–5.77 (m, 1H), 4.60–4.58 (m, 1H), 4.27–4.18 (m, 2H), 4.07–4.00 (m, 2H), 3.89–3.86 (m, 1H), 2.92–2.82 (m, 2H), 2.59–2.56 (m, 2H), 1.74 (t,  $J = 7.2$  Hz, 2H), 1.30–1.21 (m, 4H), 0.97–0.89 (m, 4H); MS  $m/z$ :  $[\text{M} + \text{H}]^+$  502; HRMS ( $m/z$ ):  $[\text{M} + \text{H}]^+$  calcd for  $\text{C}_{29}\text{H}_{36}\text{N}_5\text{O}_3$ , 502.2813; found, 502.2808.

**4.2.24.4. 6-(7-Oxa-macrocyclic-1-yl)-N-hydroxy-6-oxohexanamide (33).**  $^1\text{H NMR}$  (400 MHz,  $\text{DMSO}-d_6$ ,  $\delta$ ): 10.34 (br, 1H), 9.79 (d,  $J = 4.0$  Hz, 1H), 8.58 (s, 1H), 8.56 (d,  $J = 5.2$  Hz, 1H), 7.87 (br, 1H), 7.68–7.65 (m, 1H), 7.47 (t,  $J = 8.0$  Hz, 1H), 7.44–7.41 (m, 1H), 7.31–7.22 (m, 2H), 7.08 (d,  $J = 8.0$  Hz, 1H), 6.68 (d,  $J = 7.6$  Hz, 1H), 5.60–5.53 (m, 1H), 5.46–5.41 (m, 1H), 4.66 (s, 1H), 4.60 (s, 1H), 4.19–4.16 (m, 2H), 3.97–3.95 (m, 1H), 3.85–3.83 (m, 1H), 2.45–2.43 (m, 4H), 1.98–1.95 (m, 2H), 1.55–1.51 (m, 4H); MS  $m/z$ :  $[\text{M} + \text{H}]^+$  502; HRMS ( $m/z$ ):  $[\text{M} + \text{H}]^+$  calcd for  $\text{C}_{28}\text{H}_{32}\text{N}_5\text{O}_4$ , 502.2449; found, 502.2450.

**4.2.24.5. 8-(7-Oxa-macrocyclic-1-yl)-N-hydroxy-8-oxooctanamide (34).**  $^1\text{H NMR}$  (400 MHz,  $\text{DMSO}-d_6$ ,  $\delta$ ): 10.34 (br, 1H), 9.79 (s, 1H), 8.58 (s, 1H), 8.56 (d,  $J = 5.2$  Hz, 1H), 7.87 (br, 1H), 7.68–7.65 (m, 1H), 7.47 (t,  $J = 8.0$  Hz, 1H), 7.44–7.41 (m, 1H), 7.31–7.23 (m, 2H), 7.08 (d,  $J = 8.0$  Hz, 1H), 6.69–6.67 (m, 1H), 5.60–5.54 (m, 1H), 5.44–5.37 (m, 1H), 4.66 (s, 1H), 4.60 (s, 1H), 4.19–4.16 (m, 2H), 3.97–3.95 (m, 1H), 3.85–3.83 (m, 1H), 2.45–2.39 (m, 4H), 1.96–1.91 (m, 2H), 1.56–1.46 (m, 4H), 1.28–1.23 (m, 4H); MS  $m/z$ :  $[\text{M} + \text{H}]^+$  530; HRMS ( $m/z$ ):  $[\text{M} + \text{H}]^+$  calcd for  $\text{C}_{30}\text{H}_{36}\text{N}_5\text{O}_4$ , 530.2762; found, 530.2743.

**4.2.24.6. 9-(7-Oxa-macrocyclic-1-yl)-N-hydroxy-9-oxononamide (35).**  $^1\text{H NMR}$  (400 MHz,  $\text{DMSO}-d_6$ ,  $\delta$ ): 10.34 (br, 1H), 9.78 (s, 1H), 8.58 (s, 1H), 8.56 (d,  $J = 5.2$  Hz, 1H), 7.87 (t,  $J = 2.0$  Hz, 1H), 7.68–7.65 (m, 1H), 7.47 (t,  $J = 8.0$  Hz, 1H), 7.42 (t,  $J = 5.6$  Hz, 1H), 7.31–7.22 (m, 2H), 7.08 (d,  $J = 8.0$  Hz, 1H), 6.69–6.66 (m, 1H), 5.60–5.53 (m, 1H), 5.40–5.32 (m, 1H), 4.66 (s, 1H), 4.60 (s, 1H), 4.19–4.16 (m, 2H), 3.97–3.96 (m, 1H), 3.85–3.84 (m, 1H), 2.44–2.40 (m, 4H), 1.96–1.89 (m, 2H), 1.56–1.45 (m, 4H), 1.28–1.22 (m, 6H); MS  $m/z$ :  $[\text{M} + \text{H}]^+$  544; HRMS ( $m/z$ ):  $[\text{M} + \text{H}]^+$  calcd for  $\text{C}_{31}\text{H}_{38}\text{N}_5\text{O}_4$ , 544.2918; found, 544.2900.

**4.2.24.7. 5-(6-Oxa-macrocyclic-1-yl)-N-hydroxypentanamide (36).**  $^1\text{H NMR}$  (400 MHz,  $\text{DMSO}-d_6$ ,  $\delta$ ): 10.40 (br, 1H), 9.98 (s, 1H), 9.68 (br, 1H), 8.78 (s, 1H), 8.61 (d,  $J = 5.2$  Hz, 1H), 8.33 (s, 1H), 8.09–8.07 (m, 1H), 7.61–7.58 (m, 2H), 7.53 (d,  $J = 5.2$  Hz, 1H), 7.41 (t,  $J = 8.0$  Hz, 1H), 7.32 (d,  $J = 8.0$  Hz, 1H), 7.16 (d,  $J = 7.2$  Hz, 1H), 6.22–6.16 (m, 1H), 5.93–5.82 (m, 1H), 4.46–4.11 (m, 4H), 3.94–3.93 (m, 1H), 3.83–3.82 (m, 1H), 3.01–2.95 (m, 2H), 1.95 (t,  $J = 7.2$  Hz, 2H), 1.77–1.41 (m, 4H); MS  $m/z$ :  $[\text{M} + \text{H}]^+$  474; HRMS ( $m/z$ ):  $[\text{M} + \text{H}]^+$  calcd for  $\text{C}_{27}\text{H}_{32}\text{N}_5\text{O}_3$ , 474.2500; found, 474.2487.

**4.2.24.8. 6-(6-Oxa-macrocyclic-1-yl)-N-hydroxyhexanamide (37).**  $^1\text{H NMR}$  (400 MHz,  $\text{DMSO}-d_6$ ,  $\delta$ ): 10.36 (br, 1H), 9.98 (s, 1H), 9.65 (br, 1H), 8.78 (s, 1H), 8.61 (d,  $J = 5.2$  Hz, 1H), 8.32 (s, 1H), 8.09–8.07 (m, 1H), 7.60–7.58 (m, 2H), 7.53 (d,  $J = 5.2$  Hz, 1H), 7.40 (t,  $J = 8.0$  Hz, 1H), 7.31 (d,  $J = 8.0$  Hz, 1H), 7.16 (d,  $J = 7.2$  Hz, 1H), 6.22–6.16 (m, 1H), 5.93–5.85 (m, 1H), 4.62–4.56 (m, 2H), 4.46–4.36 (m, 2H), 4.14–4.11 (m, 2H), 3.95–3.94 (m, 1H), 3.81–3.80 (m, 1H), 2.98–2.91 (m, 2H), 1.92 (t,  $J = 7.2$  Hz, 2H), 1.81–1.42 (m, 4H), 1.23–1.18 (m, 2H); MS  $m/z$ :  $[\text{M} + \text{H}]^+$  488; HRMS ( $m/z$ ):  $[\text{M} + \text{H}]^+$  calcd for  $\text{C}_{28}\text{H}_{32}\text{N}_5\text{O}_3$ , 488.2656; found, 488.2662.

**4.2.24.9. 7-(6-Oxa-macrocyclic-1-yl)-N-hydroxyheptanamide (38).**  $^1\text{H NMR}$  (400 MHz,  $\text{DMSO}-d_6$ ,  $\delta$ ): 10.34 (br, 1H), 9.97 (s, 1H), 9.69 (br, 1H), 8.78 (s, 1H), 8.61 (d,  $J = 5.2$  Hz, 1H), 8.33 (s, 1H), 8.09–8.07 (m, 1H), 7.60–7.58 (m, 2H), 7.53 (d,  $J = 5.2$  Hz, 1H), 7.41 (t,  $J = 8.0$  Hz, 1H), 7.31 (d,  $J = 8.0$  Hz, 1H), 7.16 (d,  $J = 7.2$  Hz, 1H), 6.21–6.16 (m, 1H), 5.92–5.89 (m, 1H), 4.61–4.58 (m, 2H), 4.45–4.11 (m, 4H), 3.95–3.94 (m, 1H), 3.82–3.81 (m, 1H), 2.99–2.92 (m, 2H), 1.91 (t,  $J = 7.2$  Hz, 2H), 1.76–1.43 (m, 4H), 1.19 (br, 4H); MS  $m/z$ :  $[\text{M} + \text{H}]^+$  502; HRMS ( $m/z$ ):  $[\text{M} + \text{H}]^+$  calcd for  $\text{C}_{29}\text{H}_{36}\text{N}_5\text{O}_3$ , 502.2813; found, 502.2791.

**4.2.24.10. 6-(6-Oxa-macrocyclic-1-yl)-N-hydroxy-6-oxohexanamide (39).**  $^1\text{H NMR}$  (400 MHz,  $\text{Acetone}-d_6$ ,  $\delta$ ): 9.80 (s, 1H), 8.68 (br, 1H), 8.61 (s, 1H), 8.50 (d,  $J = 5.2$  Hz, 1H), 8.44 (s, 1H), 8.03 (s, 1H), 7.80 (br, 1H), 7.60–7.52 (m, 2H), 7.43 (d,  $J = 5.2$  Hz, 1H), 7.25 (t,  $J = 7.6$  Hz, 1H), 7.13 (d,  $J = 8.0$  Hz, 1H), 6.99 (d,  $J = 6.8$  Hz, 1H), 5.84–5.68 (m, 2H), 4.61 (s, 2H), 3.96 (d,  $J = 4.8$  Hz, 2H), 3.64 (s, 1H), 3.16 (d,  $J = 6.0$  Hz, 2H), 2.39 (t,  $J = 7.2$  Hz, 2H), 2.04 (t,  $J = 7.2$  Hz, 2H), 1.50–1.43 (m, 3H); MS  $m/z$ :  $[\text{M} + \text{H}]^+$  502; HRMS ( $m/z$ ):  $[\text{M} + \text{H}]^+$  calcd for  $\text{C}_{28}\text{H}_{32}\text{N}_5\text{O}_4$ , 502.2449; found, 502.2431.

**4.2.24.11. 8-(6-Oxa-macrocyclic-1-yl)-N-hydroxy-8-oxooctanamide (40).**  $^1\text{H NMR}$  (400 MHz,  $\text{DMSO}-d_6$ ,  $\delta$ ): 10.43 (s, 2H), 10.01 (d,  $J = 3.2$  Hz, 1H), 8.61 (s, 1H), 8.60 (d,  $J = 5.2$  Hz, 1H), 8.31 (d,  $J = 8.0$  Hz, 1H), 8.08 (br, 1H), 7.55–7.52 (m, 3H), 7.35–7.31 (m, 1H), 7.17 (t,  $J = 7.6$  Hz, 1H), 6.71 (d,  $J = 7.6$  Hz, 1H), 5.69–5.62 (m, 2H), 4.65–4.49 (m, 4H), 3.99 (m, 3H), 3.89 (m, 1H), 2.48–2.42 (m, 2H), 1.98–1.93 (m, 2H), 1.57–1.45 (m, 4H), 1.29–1.24 (m, 4H); MS  $m/z$ :  $[\text{M} + \text{H}]^+$  530; HRMS ( $m/z$ ):  $[\text{M} + \text{H}]^+$  calcd for  $\text{C}_{30}\text{H}_{36}\text{N}_5\text{O}_4$ , 530.2761; found, 530.2765.

**4.2.24.12. 9-(6-Oxa-macrocyclic-1-yl)-N-hydroxy-9-oxononamide (41).**  $^1\text{H NMR}$  (400 MHz,  $\text{DMSO}-d_6$ ,  $\delta$ ): 10.35 (br, 1H), 9.85 (s, 1H),

8.66 (br, 1H), 8.58 (dd,  $J = 5.2$  Hz,  $J = 1.6$  Hz, 1H), 8.32 (d,  $J = 7.6$  Hz, 1H), 8.07–8.05 (m, 1H), 7.54–7.45 (m, 3H), 7.30–7.27 (m, 1H), 7.15 (t,  $J = 7.2$  Hz, 1H), 6.89 (d,  $J = 7.2$  Hz, 1H), 5.76–5.67 (m, 1H), 5.63–5.61 (m, 1H), 4.64 (br, 2H), 4.51–4.87 (m, 2H), 3.99–3.98 (m, 3H), 3.88–3.87 (m, 1H), 2.48–2.42 (m, 2H), 1.96–1.91 (m, 2H), 1.58–1.45 (m, 4H), 1.29–1.24 (m, 6H); MS  $m/z$ :  $[M + H]^+$  544; HRMS ( $m/z$ ):  $[M + H]^+$  calcd for  $C_{31}H_{38}N_5O_4$ , 544.2918; found, 544.2899.

#### 4.3. HDAC inhibition assay

The HDAC inhibitory activities were assessed using the Biomol Fluor de Lys assay kit (AK-500, Enzo Life Sciences, Inc.), as previously described by us [20,21]. Briefly, HeLa cell nuclear extracts were incubated with test compounds, and HDAC reaction was initiated by addition of Fluor de Lys substrate. The resulting mixture was incubated for 2 h at room temperature, followed by adding developer to stop the reaction. Fluorescence was measured by a microplate reader (SpectraMax M5) with excitation at 360 nm and emission at 460 nm.

#### 4.4. FLT3 kinase assay

FLT3 kinase activities were measured using LanthaScreen™ assay platform (Invitrogen) according to the manufacturer's instructions. Briefly, the time-resolved fluorescence energy transfer (TR-FRET) assay was performed in white, low-volume 384-well plates (Corning Part#3673). The recombinant enzyme FLT3 (catalog no.PV3182, Invitrogen) was incubated with LanthaScreen™ Eu-anti-His antibody, Alexa Fluor 647-labeled kinase tracer 236 and various concentrations of tested compounds for 1 h at room temperature. Then, the single was measured at 665/615 nm emission ratio on a microplate reader (SpectraMax M5).

#### 4.5. JAK2 kinase assay

JAK2 kinase activities were determined using Z'-LYTE™ kinase assay platform (Invitrogen). The assay was carried out in black, low-volume 384-well plates (Corning Part#3676). Briefly, in a 10  $\mu$ L kinase reaction, each well contains 30 ng/mL JAK2 (catalog no.PV4210, Invitrogen), 4  $\mu$ M Z'-LYTE Try6 peptide substrate, 25  $\mu$ M ATP and various concentrations of tested compounds. The kinase reaction was performed at room temperature for 1 h. Then, development reagent was added into each well. After additional 1 h incubation at room temperature, stop reagent was added to halt the development reaction. The single was measured at 445/520 nm emission ratio on a microplate reader (SpectraMax M5e).

#### 4.6. Cell proliferation assay

The anti-proliferative activities were measured using SRB assay or ATP content assay. Briefly, cells, obtained from the American Type Culture Collection (ATCC, Manassas, VA), were seeded at 2000–5000 cells/well in 96-well plates and maintained for 24 h. The cells were then treated with various concentrations of test compounds for 48 h. Cell viability was monitored using Sulforhodamine B dye (SRB, Sigma–Aldrich) or CellTiter-Glo Assay kit (Promega, Madison, WI, USA). Finally the absorbance or luminescence was measured on a microplate reader (SpectraMax M5) according to the manufacturer.

#### 4.7. Western blotting

For western blotting, cells were plated at  $0.2 \times 10^6$  mL<sup>-1</sup> in the presence or absence of various concentrations of tested compounds. After incubated for 24 h, cells were collected and lysed in a

whole cell lysis buffer (Beyotime, #p0013). SDS-polyacrylamide gel electrophoresis and western blotting were performed according to the standard procedures using total cellular extracts. Antibodies against acetylated histone H3 (#06-599) were obtained from Millipore, antibodies against acetylated tubulin (T7451) and tubulin (T6199) were obtained from Sigma–Aldrich, and antibodies against phosphor-FLT3 Y591 (#3461), phosphor-JAK2 Y1007/1008 (#3776), phosphor-STAT5 Y694 (#3939) and phosphor-AKT T308 (#4056) were obtained from Cell Signaling Technologies. Detection was performed using horse-radish peroxidase-labeled secondary antibodies (Santa Cruz).

#### 4.8. Molecular modeling

Protein complexes were obtained directly from protein data bank (PDB). For HDLP (PDB code: 1C3S) and JAK2 (PDB code: 2B7A), all waters were eliminated and one chain was retained. Hydrogen and partial charges were added through protonate 3D program of MOE. Default parameter settings generated by the program dock of MOE were used for docking. For FLT3, the FLT3 X-ray structure (PDB code: 1RJB) obtained from PDB is in the DFG-out conformation that prevents our inhibitors from being docked into the ATP-binding site. Thus, an X-ray/homology model of DFG-in conformation of FLT3 was constructed based on FGFR2 X-ray structure (PDB code: 1OEC) according to the method described by Poulsen using homology model program of MOE [25]. Then, the protein preparation and ligand-docking were accomplished as previously described.

#### Acknowledgments

We thank the National Natural Science Foundation of China for financial support (Project Number: 30873137, 30772645 and 81172927).

#### Appendix A. Supplementary data

Supplementary data related to this article can be found at <http://dx.doi.org/10.1016/j.ejmech.2015.03.034>.

#### References

- [1] B. Löwenberg, J.R. Downing, A. Burnett, Acute myeloid leukemia, *N. Engl. J. Med.* 341 (1999) 1051–1062.
- [2] J.L. Shipley, J.N. Butera, Acute myelogenous leukemia, *Exp. Hematol.* 37 (2009) 649–659.
- [3] J. Felipe Rico, D.C. Hassane, M.L. Guzman, Acute myelogenous leukemia stem cells: from Bench to Bedside, *Cancer Lett.* 338 (2013) 4–9.
- [4] A. Kuendgen, U. Germing, Emerging treatment strategies for acute myeloid leukemia (AML) in the elderly, *Cancer Treat. Rev.* 35 (2009) 97–120.
- [5] J.A. Zwiebel, New agents for acute myelogenous leukemia, *Leukemia* 14 (2000) 488–490.
- [6] L.M. LaFave, R.L. Levine, JAK2 the future: therapeutic strategies for JAK-dependent malignancies, *Trends Pharmacol. Sci.* 33 (2012) 574–582.
- [7] P. Marks, R.A. Rifkind, V.M. Richon, R. Breslow, T. Miller, W.K. Kelly, Histone deacetylases and cancer: causes and therapies, *Nat. Rev. Cancer* 1 (2001) 194–202.
- [8] J.E. Bolden, M.J. Peart, R.W. Johnstone, Anticancer activities of histone deacetylase inhibitors, *Nat. Rev. Drug Discov.* 5 (2006) 769–784.
- [9] P. Gallinari, S. Di Marco, P. Jones, M. Pallaoro, C. Steinkühler, HDACs, histone deacetylation and gene transcription: from molecular biology to cancer therapeutics, *Cell. Res.* 17 (2007) 195–211.
- [10] X. Cai, H.X. Zhai, J. Wang, J. Forrester, H. Qu, L. Yin, C.J. Lai, R. Bao, C. Qian, Discovery of 7-(4-(3-ethynylphenylamino)-7-methoxyquinazolin-6-yloxy)-N-hydroxyheptanamide (CUDc-101) as a potent multi-acting HDAC, EGFR, and HER2 inhibitor for the treatment of cancer, *J. Med. Chem.* 53 (2010) 2000–2009.
- [11] M. Beffinger, A. Skwarska, The role of FLT3 kinase as an AML therapy target, *Curr. Pharm. Des.* 18 (2012) 2758–2765.
- [12] M. Buchwald, K. Pietschmann, J.P. Müller, F.D. Böhmer, T. Heinzel, O.H. Krämer, Ubiquitin conjugase UBCH8 targets active FMS-like tyrosine kinase 3 for proteasomal degradation, *Leukemia* 24 (2010) 1412–1421.
- [13] S.G. Rane, E.P. Reddy, Janus kinases: components of multiple signaling

- pathways, *Oncogene* 19 (2000) 5662–5679.
- [14] A. Quintás-Cardama, The role of Janus kinase 2 (JAK2) in myeloproliferative neoplasms: therapeutic implications, *Leuk. Res.* 37 (2013) 465–472.
- [15] J.W. Lee, Y.G. Kim, Y.H. Soung, K.J. Han, S.Y. Kim, H.S. Rhim, W.S. Min, S.W. Nam, W.S. Park, J.Y. Lee, N.J. Yoo, S.H. Lee, The JAK2 V617F mutation in de novo acute myelogenous leukemias, *Oncogene* 25 (2006) 1434–1436.
- [16] Y. Wang, W. Fiskus, D.G. Chong, K.M. Buckley, K. Natarajan, R. Rao, A. Joshi, R. Balusu, S. Koul, J. Chen, A. Savoie, C. Ustun, A.P. Jillella, P. Atadja, R.L. Levine, K.N. Bhalla, Cotreatment with panobinostat and JAK2 inhibitor TG101209 attenuates JAK2<sup>V617F</sup> levels and signaling and exerts synergistic cytotoxic effects against human myeloproliferative neoplastic cells, *Blood* 114 (2009) 5024–5033.
- [17] V. Novotny-Diermayr, S. Hart, K.C. Goh, A. Cheong, L.C. Ong, H. Hentze, M.K. Pasha, R. Jayaraman, K. Ethirajulu, J.M. Wood, The oral HDAC inhibitor pracinostat (SB939) is efficacious and synergistic with the JAK2 inhibitor pacritinib (SB1518) in preclinical models of AML, *Blood Cancer J.* 2 (2012) e69.
- [18] C. Nishioka, T. Ikezoe, J. Yang, S. Takeuchi, H.P. Koeffler, A. Yokoyama, MS-275, a novel histone deacetylase inhibitor with selectivity against HDAC1, induces degradation of FLT3 via inhibition of chaperone function of heat shock protein 90 in AML cells, *Leuk. Res.* 32 (2008) 1382–1392.
- [19] M.S. Finnin, J.R. Donigian, A. Cohen, V.M. Richon, R.A. Rifkind, P.A. Marks, R. Breslow, N.P. Pavletich, Structures of a histone deacetylase homologue bound to the TSA and SAHA inhibitors, *Nature* 401 (1999) 188–193.
- [20] M. Zhou, C. Ning, R. Liu, Y. He, N. Yu, Design, synthesis and biological evaluation of indeno[1,2-d]thiazole derivatives as potent histone deacetylase inhibitors, *Bioorg. Med. Chem. Lett.* 23 (2013) 3200–3203.
- [21] C. Ning, Y. Bi, Y. He, W. Huang, L. Liu, Y. Li, S. Zhang, X. Liu, N. Yu, Design, synthesis and biological evaluation of di-substituted cinnamic hydroxamic acids bearing urea/thiourea unit as potent histone deacetylase inhibitors, *Bioorg. Med. Chem. Lett.* 23 (2013) 6432–6435.
- [22] A.D. William, A.C.H. Lee, S. Blanchard, A. Poulsen, E.L. Teo, H. Nagaraj, E. Tan, D. Chen, M. Williams, E.T. Sun, K.C. Goh, W.C. Ong, S.K. Goh, S. Hart, R. Jayaraman, M.K. Pasha, K. Ethirajulu, J.M. Wood, B.W. Dymock, Discovery of the Macrocycle 11-(2-Pyrrolidin-1-yl-ethoxy)-14,19-dioxa-5,7,26-triaza-tetracyclo[19.3.1.1(2,6).1(8,12)]heptacosa-1(25),2(26),3,5,8,10,12(27),16,21,23-decaene (SB1518), a Potent Janus Kinase 2/Fms-Like Tyrosine Kinase-3 (JAK2/FLT3) Inhibitor for the Treatment of Myelofibrosis and Lymphoma, *J. Med. Chem.* 54 (2011) 4638–4658.
- [23] A.D. William, A.C.H. Lee, K.C. Goh, S. Blanchard, A. Poulsen, E.L. Teo, H. Nagaraj, C.P. Lee, H. Wang, M. Williams, E.T. Sun, C. Hu, R. Jayaraman, M.K. Pasha, K. Ethirajulu, J.M. Wood, B.W. Dymock, Discovery of kinase spectrum selective macrocycle (16E)-14-methyl-20-oxa-5,7,14,26-tetraazatetracyclo[19.3.1.1(2,6).1(8,12)]heptacosa-1(25),2(26),3,5,8(27),9,11,16,21,23-decaene (SB1317/TG02), a potent inhibitor of cyclin dependent kinases (CDKs), janus kinase 2 (JAK2), and Fms-like tyrosine kinase-3 (FLT3) for the treatment of Cancer, *J. Med. Chem.* 55 (2012) 169–196.
- [24] D.Y. Ma, N.F. Yu, Synthesis of novel 2-(substituted anilino)pyrimidine derivatives, *Chin. J. Org. Chem.* 28 (2008) 1448–1453.
- [25] A. Poulsen, A. William, S. Blanchard, H. Nagaraj, M. Williams, H. Wang, A. Lee, E. Sun, E.L. Teo, E. Tan, K.C. Goh, B. Dymock, Structure-based design of nitrogen-linked macrocyclic kinase inhibitors leading to the clinical candidate SB1317/TG02, a potent inhibitor of cyclin dependant kinases (CDKs), Janus kinase 2 (JAK2), and Fms-like tyrosine kinase-3 (FLT3), *J. Mol. Model* 19 (2013) 119–130.